Journal of Non-Crystalline Solids 353 (2007) 2237–2243

Crystallization kinetics of $1Na_2O \cdot 2CaO \cdot 3SiO_2 \cdot$ glass monitored by electrical conductivity measurements

Ana Candida M. Rodrigues [a,*], Gilberto Tadashi Niitsu [a], Edgar Dutra Zanotto [a], Miguel Oscar Prado [b], Vladimir Fokin [c]

[a] *Laboratório de Materiais Vítreos, Departamento de Engenharia de Materiais, Universidade Federal de São Carlos, C.P. 676 -13565-905 São Carlos, SP, Brazil*
[b] *Comisión Nacional de Energía Atómica-Centro Atómico Bariloche-8400 S.C. de Bariloche (RN), Argentina*
[c] *S.I. Vavilov's State Optical Institute, Babushkina 36/1, St. Petersburg 193171, Russia*

Received 2 July 2006; received in revised form 18 January 2007
Available online 1 May 2007

Abstract

We investigated the kinetics of crystal nucleation, growth, and overall crystallization of a glass with composition close to the stoichiometric $1Na_2O \cdot 2CaO \cdot 3SiO_2$. The nucleation and subsequent growth of sodium-rich crystals in this glass decreases the sodium content in the glassy matrix, drastically hindering further nucleation and growth. Compositional changes of the crystals and glassy matrix at different stages of the crystallization process were determined by EDS. These compositional variations were also monitored by electrical conductivity measurements, carried out by impedance spectroscopy, in glassy, partially, and fully crystallized samples. The electrical conductivity of both crystalline and glassy phases decreases with the increase of the crystallized volume fraction. Starting at a crystallized volume fraction of about 0.5, the crystalline phase dominates the electrical conductivity of the sample. This behavior was corroborated by an analysis of the activation energy for conduction. We show that electrical conductivity is highly sensitive and can indicate compositional shifts, changes in the spatial distribution of mobile ions in the glassy matrix. Conductivity measurements are thus a powerful tool for the investigation of complex heterogeneous systems, such as partially crystallized glasses and glass-ceramics.

PACS: 72.80.Ng; 64.70.Dv

Keywords: Crystal growth; Glass-ceramics; Nucleation; Conductivity; Oxide glasses; Soda-lime-silica

1. Introduction

The understanding of the properties of multiphase systems is one of the challenging problems of modern materials science, and partially crystallized glasses and glass-ceramics are important multiphase systems. In most systems, the composition of the embedded crystals differs from those of the parent glasses, which complicates the crystallization pathways. As some of us have recently shown [1], this situation may take place even in the case of stoichiometric glass crystallization, or crystallization of glasses belonging to a compositional interval of solid solution formation, when fully crystallized samples have a single phase with the parent glass composition. The deviation of the critical nuclei's composition from that of the stable phase has been interpreted [1] as resulting from a decrease of the thermodynamic barrier for nucleation as compared with that for nuclei that have the stable phase composition. This interpretation is consistent with Ostwald's rule of stages, generalized in Ref. [2] for nucleation as '*Those classes of critical clusters determine the process of the transformation, which correspond to a minimum work of critical cluster formation (as compared with all other*

* Corresponding author. Tel.: +55 16 33518524.
E-mail address: acmr@power.ufscar.br (A.C.M. Rodrigues).

0022-3093/$ - see front matter © 2007 Elsevier B.V. All rights reserved.
doi:10.1016/j.jnoncrysol.2007.03.015

possible alternative structures and compositions, which may be formed at the given thermodynamic constraints)'. Nucleation and the deterministic growth of crystals with shifted compositions result in a simultaneous change of the glassy matrix composition, as shown experimentally for a series of sodium-calcium-silicate glasses belonging to the $1Na_2O \cdot 2CaO \cdot 3SiO_2(N_1C_2S_3) - 1Na_2O \cdot 1CaO \cdot 2SiO_2(N_1C_1S_2)$ pseudo-binary line [1,3]. Such complex crystallization pathway accompanied by compositional variations in the crystals and glassy matrix, and their high sodium content make these glasses quite attractive for electrical conductivity investigations.

This paper presents and discusses some relevant aspects of the crystallization kinetics of a near-stoichiometric $N_1C_2S_3$ glass from the parent to fully crystallized glass (glass-ceramic) as followed by electrical conductivity measurements, using impedance spectroscopy, and EDS.

2. Experimental and methods

2.1. Glass and glass-ceramics preparation

A $17.0Na_2O \cdot 33.2CaO \cdot 49.8SiO_2$ (mol%) glass – by analysis – was prepared from sodium and calcium carbonates, and crushed quartz by melting in a platinum crucible at 1300–1500 °C for about 4 h and casting on massive metallic plates. To obtain samples with different crystallized volume fractions, α, samples of the parent glass were heat-treated at $T = 690$ °C for different periods of time. The α values were estimated by standard methods using optical microscopy.

2.2. Crystallization kinetics

To calculate the steady-state nucleation rate, I_{st}, and time lag for nucleation, τ, for a given temperature, T, the number density of nucleated crystals, N, versus heat treatment time, t, at T was obtained by the 'development' method [3]. These data were fitted to the Collins–Kashchiev Eq. (1) to estimate I_{st} and τ as fit parameters [4].

$$N(t) = I_{st}\tau\left[\frac{t}{\tau} - \frac{\pi^2}{6} - 2\sum_{m=1}^{\infty}\frac{(-1)^m}{m^2}\exp\left(-m^2\frac{t}{\tau}\right)\right]. \quad (1)$$

The kinetics of overall crystallization were analyzed by the Avrami equation [4]

$$\alpha(t) = 1 - \exp\{-Kt^n\}, \quad (2)$$

where K is a parameter that comprises the crystal nucleation rate (or the crystal number density) and the growth rate, n is the Avrami coefficient, which in the case of the three-dimensional growth can be approximately written as

$$n = k + 3\,m. \quad (3)$$

k and m are exponents of t in the formulas $N \sim t^k$ and $D \sim t^m$ describing the variations of the crystal number (N) and size (D) with time [3].

2.3. Estimates of the crystals and glassy matrix compositions

The average compositions of the crystals were analyzed by EDS using a fully crystallized sample as a standard. The composition of the glassy matrix was then calculated based on the parent glass and crystal compositions taking into account the values of α.

2.3.1. Impedance spectroscopy

Electrical conductivity measurements were carried out by impedance spectroscopy, which employs alternating current with variable frequency. The main feature of this method, which is widely employed in investigations of semiconductors and ionic conductors, is that it allows for the separation of electrical phenomena having different time constants, e.g., electrode and bulk properties [5]. Impedance data of a homogeneous ionic conducting glass, can be represented by a so-called Nyquist diagram (x-axis: the real part of the impedance; y-axis: the negative of the imaginary part of impedance), which is commonly a semi-circle followed by a characteristic spike of electrode polarization due to ionic conduction. The sample's resistance (R) is read at the intersection of the semi-circle with the x-axis at low frequencies. The electrical conductivity, σ, can thus easily be calculated employing:

$$\sigma = \frac{1}{R}\frac{L}{S}, \quad (4)$$

where L is the sample's thickness and S the electrode surface area.

Before taking the measurements, to ensure that only bulk properties would be investigated, the crystallized surface layer was eliminated by polishing. Platinum electrodes were then sputtered onto the samples' surfaces to ensure the necessary electrical contact. Measurements were taken in a two-electrode configuration cell, in dry air, using an impedance analyzer HP 4192A, which allows the frequency to vary from a 5 Hz to 13 MHz. The measurements were done in the 250–600 °C temperature range.

3. Results

3.1. Crystallization kinetics and EDS data

Figs. 1 and 2 show a typical kinetic curve, $N(t)$, and the temperature dependencies of the steady-state nucleation rate, I_{st}, and time lag, τ, for nucleation, respectively. The overall crystallization was studied at $T = 690$ °C, which exceeds the temperature corresponding to the maximum nucleation rate $T_{max} \cong 593$ °C (see Fig. 2) by about 100 °C, and hence corresponds mainly to growth of 'athermal' crystals, i.e. crystals nucleated during cooling of the melt and heating of the glass up to the temperature under study. $T = 690$ °C was also used to prepare samples with different crystallized volume fractions. Fig. 3 shows α and the diameter of the crystals, that is equal to the largest

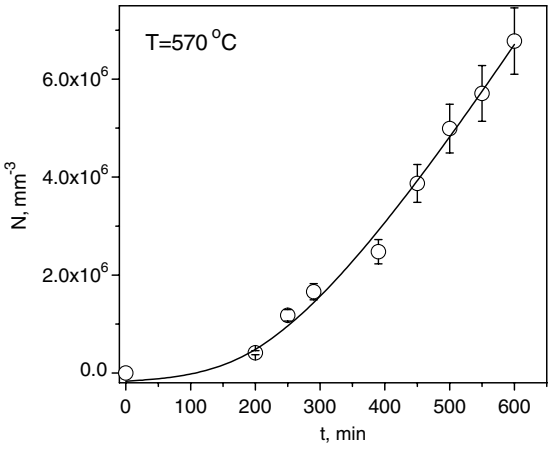

Fig. 1. The number density of crystals nucleated at $T = 570$ °C versus time. Line is plotted with Eq. (1) employing $m = 4$.

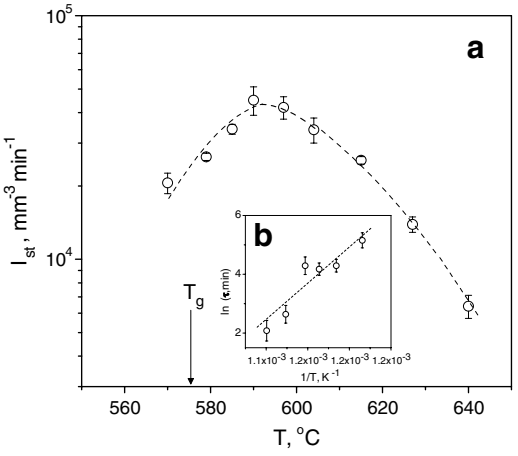

Fig. 2. Steady-state nucleation rate (a) and time lag for nucleation (b) versus temperature and inverse temperature respectively. Dashed line is placed to guide the eyes. Doted line refers to linear approximation.

crystal cross-section size on the polished surface of the sample, *versus* heat treatment time at $T = 690$ °C. The values of n and m are also shown close to the respective curves.

Fig. 4 shows the evolution of sodium and calcium contents in the crystals, and the sodium content (the main element responsible for electrical conduction) in the glassy matrix with increasing crystal volume fraction. Continuous variations in the crystal's composition are possible because the evolving crystalline phase is a solid solution with the chemical formula $Na_{4+2x}Ca_{4-x}[Si_6O_{18}]$ $(0 \leqslant x \leqslant 1)$ [6]. The crystals with x up to 0.5 reveal reversible polymorphous transition at T_{pm}, which is much lower than the glass transition temperature T_g. This phase transition is accompanied by a thermal effect well detected on DSC curves as shown in Fig. 5.

3.2. Electrical conductivity

Conductivity data of the parent glass, partially crystallized glass, and fully crystallized sample are shown as Arrhenius plots in Fig. 6. Note that the data for amorphous and fully crystallized samples are congruent with previously published data [7]. The inflection in the Arrhenius plot of the fully crystallized sample in the temperature interval 450–500 °C is caused by the above described reversible crystal phase transition. It should be noted that the magnitude of this effect depends not only on the volume fraction of crystals, but also on the sodium content in the solid solution crystals. The higher the Na content, the weaker the effect on the DSC traces reflecting the reversible phase transformation [6]. As shown below, the sodium content in the crystalline phase decreases with increasing crystallized volume fraction. Thus, the crystalline phase present in partially crystallized glass with $\alpha \sim 0.54$ has more sodium than that present in the fully crystallized one. This is the main reason why the inflection on the Arrhenius plot of the fully crystallized sample is more pronounced than that of the sample with $\alpha \sim 0.54$.

4. Discussion

According to Ref. [1], partially crystallized glasses with compositions close to $N_1C_2S_3$ are composed of solid solution crystals that are enriched in sodium as compared to the parent glass and glassy matrix. Indeed, Fig. 4 shows that, for low crystallized volume fractions, the sodium content in the crystals by far exceeds that of the parent glass, drastically exhausting the sodium ions in the glassy matrix. Then, in the course of crystallization, the crystal composition approaches that of the parent glass.

The kinetics of overall crystallization corroborates the difference between crystal and glassy matrix compositions. According to Fig. 3 the phase transformation at $T = 690$ °C is determined only by diffusion limited growth ($m < 1$) of the practically constant number of crystals, since the equality $n = 3$ m holds. This means that $k \cong 0$ (see Eq. (3)) and hence, as expected, $I \sim 0$, since $T = 690$ °C $> T_{max}$. It should be noted that, due to the compositional evolution, m decreases with increasing the crystallized volume fraction.

Thus, the partially crystallized glass consists of a glassy matrix with embedded, randomly dispersed, spherical, sodium-enriched crystals of approximately the same size. The differences in diameters shown in Fig. 7 are due to the crystals cross-sections that appear by SEM. The glassy matrix and crystal's compositions differ from that of the parent glass and vary during phase transformation.

To aid the analysis of the conductivity data, glasses with composition similar to those of glassy matrix and crystals found during crystallization were synthesized. Glasses containing more sodium than the $N_1C_2S_3$ composition were, furthermore, fully crystallized. These 'standard' crystals and glasses were then subjected to electrical conductivity measurements, which are shown as Arrhenius plot (Fig. 8) and (for a given temperature) as a function of their sodium content (Fig. 9). In the case of partially crystallized samples (Fig. 9), the sodium content refers to the glassy

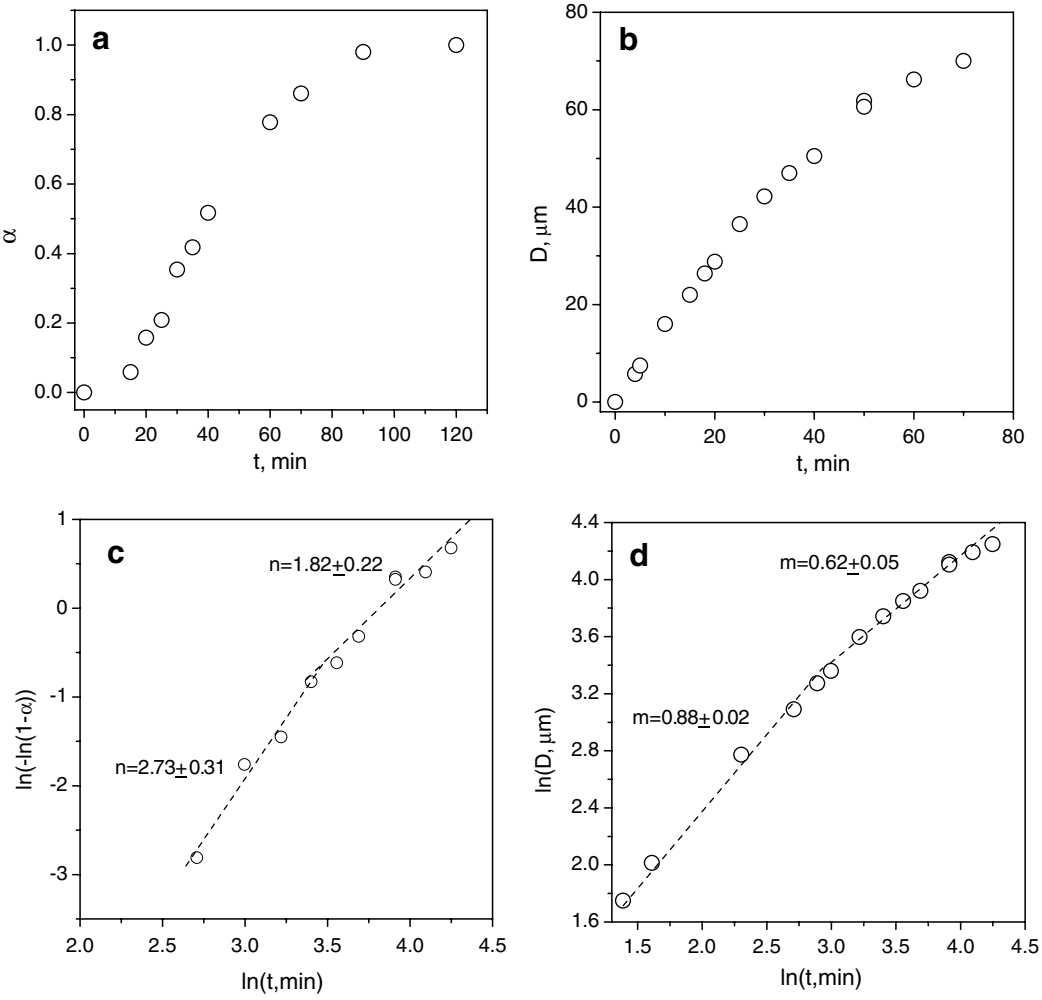

Fig. 3. Volume fraction crystallized (a, c) and diameter of largest crystals (b, d) versus time of heat treatment at $T = 690$ °C in normal (a, b), Avrami's (c), and logarithmic (d) coordinates.

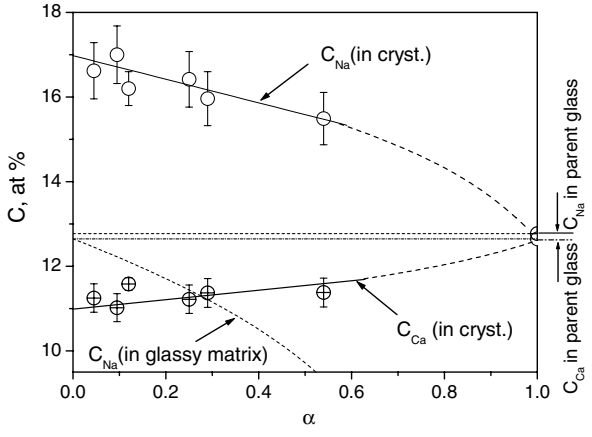

Fig. 4. Average composition, C, of the crystalline phase (points), measured by EDS, and glassy matrix, calculated from the crystallized volume fraction and the parent glass composition, *versus* volume crystallized at $T = 690$ °C.

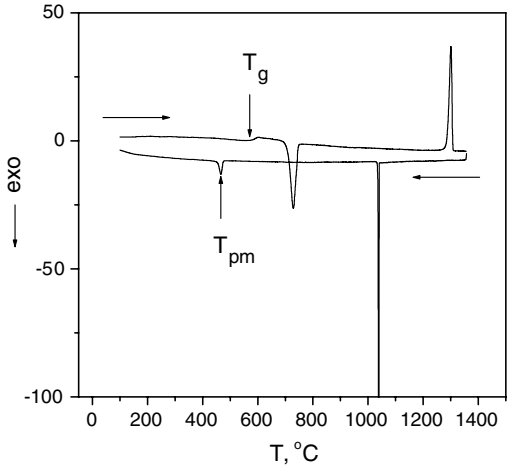

Fig. 5. DSC heating and cooling curves (heating and cooling rate of 10 °C/min) for a glass composition $17.0Na_2O \cdot 33.2CaO \cdot 49.8SiO_2$ (mol%).

matrix. At first sight, the conductivity of the partially crystallized samples, σ_{pcs}, up to $\alpha \sim 0.54$ is mainly determined by the glassy matrix, since its conductivity is close to the conductivity of the pure glass with sodium content similar

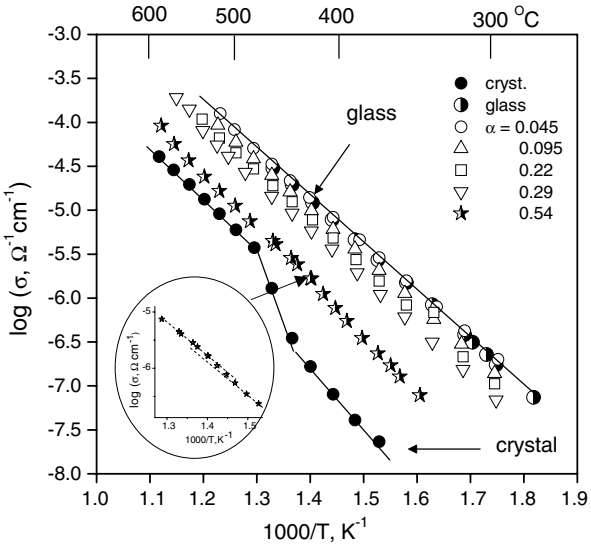

Fig. 6. Arrhenius plot of electrical conductivity of glass, partially crystallized glass, and poly-crystal.

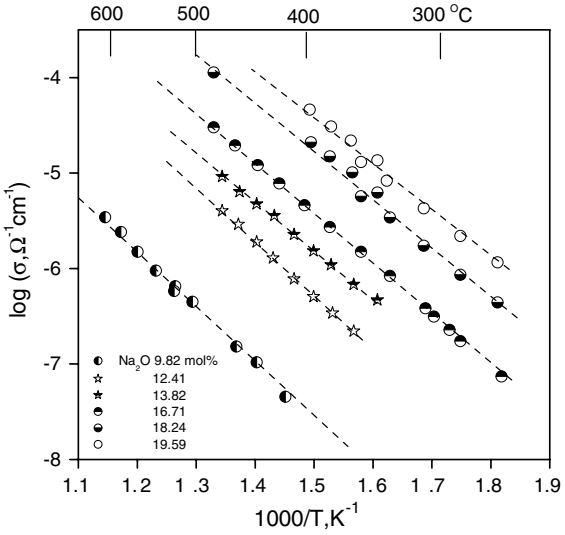

Fig. 8. Arrhenius plot of electrical conductivity of glasses with different sodium oxide content.

to that of glassy matrix (Fig. 9). However, according to Fig. 4, the crystals contain much more sodium than the respective glassy matrix, for all values of the crystallized volume fraction. As a result, the electrical conductivity of the crystals (σ_{cr}) approaches that of the glassy matrix (σ_{g-m}). Since during phase transformation the sodium content in the glassy matrix decreases faster than in crystalline phase, the electrical conductivity of the crystals becomes higher than that of the respective glassy matrix. For example, according to Fig. 4, for $\alpha \approx 0.3$ the sodium content in crystalline and glassy phases ($C_{Na}^{cr} \approx 16.15$at.%; $C_{Na}^{g-m} \approx 11.15$ at.%) corresponds at $T = 395$ °C to $\log(\sigma_{cr}) \approx -5.40$ and $\log(\sigma_{g-m}) \approx -5.70$ respectively, while for $\alpha \approx 0.54$ the conductivity of the crystalline phase ($\log(\sigma_{cr}) \approx -5.54$) exceeds that of the glassy matrix ($\log(\sigma_{g-m}) \approx -6.47$) by about one order of magnitude due to the higher difference in sodium content between crystals ($C_{Na}^{cr} \approx 15.49$ at.%) and glassy matrix ($C_{Na}^{g-m} \approx 9.32$ at.%). Hence we may assume that, beginning with $\alpha \approx 0.54$, the electrical conductivity of the sample is dominated by the crystalline phase.

To improve this analysis of the electrical conductivity of partially crystallized samples, σ_{pcs}, we calculated the respective activation energy for all samples. Such data are plotted in Fig. 10 *versus* sodium content, which refers, in the case of partly crystallized glasses, to the conductivity of the glassy matrix. Although the conductivity of the sample with $\alpha \sim 0.54$, σ_{pcs}, is close to the conductivity σ_{g-m} of a glass having the same sodium content as the glassy matrix (Fig. 9), its activation energy is higher and close to that of the sodium-enriched crystals (Fig. 10). This tendency becomes apparent at $\alpha \sim 0.30$. Thus, the comparison between the values of activation energy of partially crystallized samples, glasses, and crystals corroborate the above assumption that the electrical conductivity of partially crystallized glasses, beginning with $\alpha \sim 0.54$, is dominated by the crystals. This conclusion is reinforced by a weak inflection in the Arrhenius plot of a sample with $\alpha \sim 0.54$ (Fig. 6), which is attributed to the reversible polymorphic transition in the crystalline phase. The decrease in activation energy for conduction with the increasing of alkaline

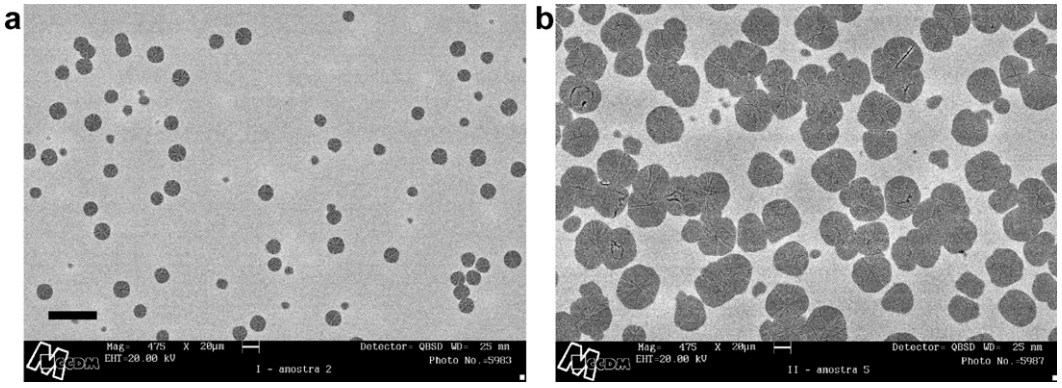

Fig. 7. SEM of the glass cross-sections treated at $T = 690$ °C for 17 (a) and 50 (b) min. Fractions of the crystallized volume are about 0.1 (a) and 0.54 (b). The bar has a length of 50 μm. The photo's height is equal to the thickness of the plates used for electrical conductivity measurement.

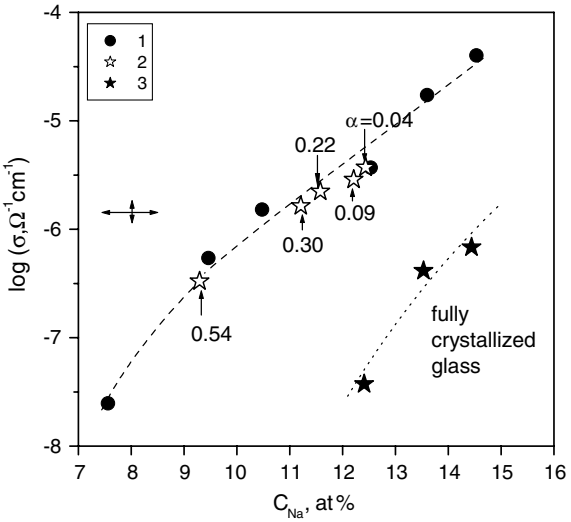

Fig. 9. Electrical conductivity at $T = 394$ °C of glasses (1), fully crystallized glasses (3) versus sodium content, and partly crystallized glass of composition close to $N_1C_2S_3$ (2) versus sodium content in the glassy matrix. The numbers close to the opened stars denote crystallized volume fraction.

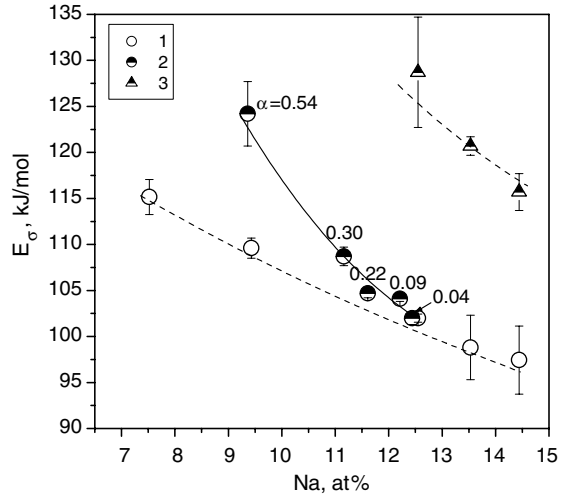

Fig. 10. Activation energy of electrical conductivity in glasses (1), partially crystallized samples (2) and crystals (3) versus sodium content. In the case of the partially crystallized glasses, sodium content corresponds to glassy matrix. The numbers close to points denote crystallized volume fractions.

content is an expected behavior for a glass system. Similar effect in the sodium calcium silicate glasses was already analyzed by Anderson and Stuart [8].

The measured and calculated compositions shown in Fig. 4 are averages. The real situation is more complicated due to the diffusion zones that exist around the growing crystals. These zones become visible with a second heat treatment at a temperature T_{n-g}, where the nucleation and growth rates are both important, since the nucleation and growth rates decrease with decreasing sodium oxide in the melt [1,9]. Indeed, as demonstrated by Fig. 11, in the areas close to the large crystals previously formed at $T = 690$ °C, and exhausted in sodium, no new crystals are

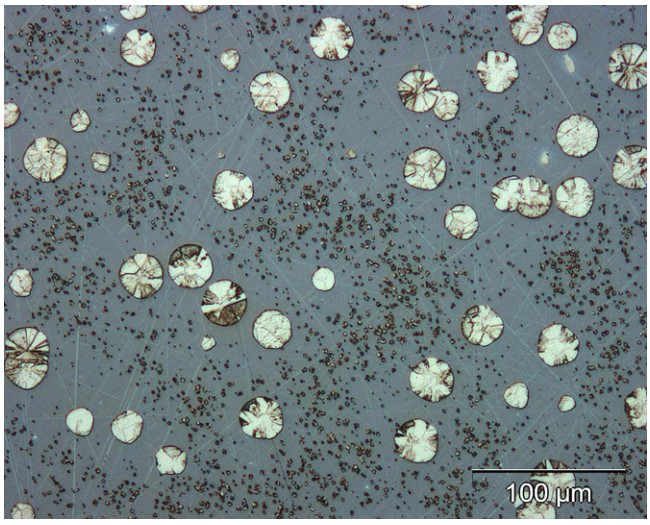

Fig. 11. Optical micrograph of glass sample subjected to the following double heat treatment: $T = 690$ °C, $t = 20$ min + $T_{n-g} = 590$ °C, $t = 17$ h. The large crystals were formed at the first heat treatment.

formed during a long heat treatment at $T_{n-g} = 590$ °C, which is close to the T_{max} (see Fig. 2). Thus, Fig. 11 presents a 'map' of sodium distribution in the glassy matrix of a sample subjected to a heat treatment at $T = 690$ °C. The areas that are distant from the large crystals form tracks enriched by sodium, which are responsible for the glassy matrix contribution to the overall conductivity of the sample. It should be noted here that crystallized volume fraction resulting from the heat treatment at $T = 690$ °C is only about 0.15. At temperatures lower than the glass transition temperature (when the crystallization process becomes too slow), sodium diffusion still occurs and the gradient of sodium concentration (see Fig. 11) must diminish resulting in a reduction of the sodium content in the above mentioned tracks, which will be gradually dissolved, thus increasing the electrical resistance of sample. It seems that this effect is the origin of the slight, but well pro-

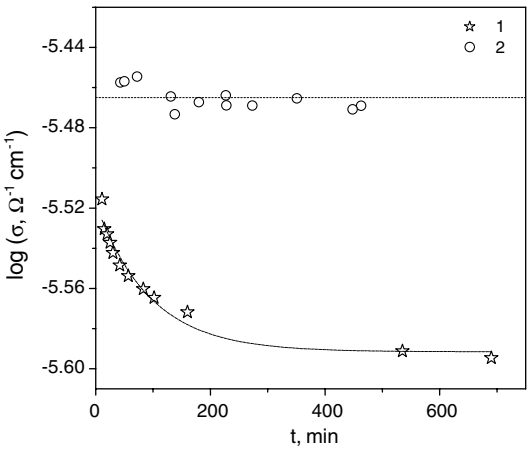

Fig. 12. Evolution of electrical conductivity at $T = 400$ °C. 1 – glass partially crystallized at $T = 690$ °C during 24 min with $\alpha \sim 0.2$; 2 – glass.

nounced decrease in the electrical conductivity of the partially crystallized sample observed during a long heat treatment at $T = 400\ ^{\circ}C$, as compared with the behavior of the pure glass (see Fig. 12).

5. Conclusions

Electrical conductivity measurements of partially crystallized samples corroborated EDS evidence for variations in the composition of both glassy phase and crystals during crystallization of a glass with composition close to the stoichiometric $1Na_2O \cdot 2CaO \cdot 3SiO_2$. In this particular case, electrical conductivity was dominated by the glassy phase up to $\alpha \sim 0.30$, and by the crystals from $\alpha \sim 0.54$. These findings were confirmed by an analysis of the electrical conductivity of glasses and crystals having the same sodium contents as the partially crystallized samples, and were further substantiated by an analysis of activation energy. For samples with higher crystallinities, Arrhenius plots showed a kink due to a crystal phase transition, confirming that the crystals dominate the electrical conductivity.

Thus, electrical conductivity is a very sensitive property that can indicate changes in the glassy matrix and crystals compositions, and in the spatial distribution of chemical elements. Hence, electrical conductivity measurements could contribute to investigations of complex heterogeneous systems, such as partially crystallized glasses.

References

[1] V.M. Fokin, O.V. Potapov, E.D. Zanotto, F.M. Spiandorello, V.L. Ugolkov, B.Z. Pevzner, J. Non-Cryst. Solids 331 (2003) 240.
[2] J.W.P. Schmelzer, J. Schmelzer Jr., I.S. Gutzow, Chem. Phys. 112 (2000) 3820.
[3] V.M. Fokin, E.D. Zanotto, N.S. Yuritsyn, J.W.P. Schmelzer, J. Non-Cryst. Solids 352 (2006) 2681.
[4] I. Gutzow, J. Schmelzer, The vitreous state, Thermodynamics, Structure, Rheology and Crystallization, Springer, Berlin, 1995.
[5] J.R. MacDonald (Ed.), Impedance Spectroscopy, Wiley, New York, 1987.
[6] I. Maki, T. Sugimura, J. Ceram. Assoc. Jpn. 75 (1968) 144.
[7] G.H. Frischat, H.L. Oel, Glastech. Ber. 39 (1966) 50.
[8] O.L. Anderson, D.A. Stuart, J. Am. Ceram. Soc. 37 (12) (1954) 573.
[9] E.N. Soboleva, N.S. Yuritsyn, V.L. Ugolkov, Glass Phys. Chem. 30 (2004) 481.